ELSEVIER

PII: S0032-3861(97)00269-3

Polymer Vol. 39 No. 10, pp. 1787–1792, 1998

0032-3861/98/$19.00+0.00

Compatibilization effect of graft copolymer on immiscible polymer blends: 1. LLDPE/SBS/LLDPE-*g*-PS systems

Hanqiao Feng[a,*], Chaohui Ye[a], Jun Tian[b], Zhiliu Feng[b] and Baotong Huang[b]

[a]*Laboratory of Magnetic Resonance and Atomic and Molecular Physics, Wuhan Institute of Physics, The Chinese Academy of Sciences, Wuhan 430071, P.R. China*

[b]*Polymer Physics Laboratory, Changchun Institute of Applied Chemistry, The Chinese Academy of Sciences, Changchun 130022, P.R. China*

(Revised 18 March 1997)

The compatibilizing effect of graft copolymer, linear low density polyethylene-*g*-polystyrene (LLDPE-*g*-PS), on immiscible blends of LLDPE with styrene–butadiene–styrene triblock copolymer (SBS) has been investigated by means of ^{13}C CPMAS n.m.r. and d.s.c. techniques. The results indicate that LLDPE-*g*-PS is an effective compatibilizer for LLDPE/SBS blends. It was found that LLDPE-*g*-PS chains connect two immiscible components, LLDPE and SBS, through solubilization of chemically identical segments of LLDPE-*g*-PS into the amorphous region of LLDPE and PS block domain of SBS, respectively. It was also found that LLDPE-*g*-PS chains connect the crystalline region of LLDPE by isomorphism, with serious effects on the supermolecular structure of LLDPE. The effect of LLDPE-*g*-PS on the supermolecular structure of LLDPE in the LLDPE/SBS blends obviously depends on the composition of the blends, but has little dependence on the PS grafting yields of LLDPE-*g*-PS. © 1998 Elsevier Science Ltd. All rights reserved.

(Keywords: ^{13}C CPMAS n.m.r.; d.s.c.; graft copolymer)

INTRODUCTION

The use of graft or block copolymers as compatibilizers for immiscible polymer blends has become an increasingly popular subject of study in recent years because it is one of the simplest and most efficient means for development of new high-performance polymer materials[1–10]. Usually, suitably chosen graft or block copolymers, whose segments may be chemically identical with those in the respective phases or miscible with one of the phases, can act as 'interfacial agents' to reduce interfacial tension and improve interfacial adhesion of the immiscible components. However, compatibilizers just located at the interfacial region may have different compatibilizing effects to those connecting two immiscible components by different chains. The former may have characteristics similar to low molecular weight emulsifiers, decreasing interfacial tension, and reducing phase growth by a steric stabilization mechanism. The latter can not only reduce interfacial tension and enhance phase stability, but also improve interfacial adhesion of the immiscible components by the 'bridge' effects of the compatibilizer chains. It is well known that interfacial adhesion is a key factor affecting the physical properties of multicomponent polymer materials with microphase separation, and hence their practical utility. The existence mode of compatibilizers in immiscible blends is the key factor affecting their compatibilizing effects. Therefore, it is a prerequisite for exploring compatibilization mechanisms to detect the existence mode of compatibilizers in blends. A lot of attention has been paid to the macroscopic effects of compatibilizers on the morphology, interfacial properties and mechanical behaviour of immiscible polymer blends. It has been assumed that compatibilizers usually locate at the interfacial region between two immiscible components, However, only a few workers[8,10] obtained direct experimental evidence by electron microscopy which supported this assumption. Even so, the evidence did not show whether or not the compatibilizers connected two immiscible components by the 'bridge' effects of the compatibilizer's chains.

Hence, the 'real' existence mode of compatibilizers in polymer blends remains unknown due to the absence of suitable detecting techniques.

It is well known that n.m.r. techniques can provide information about miscibility, molecular motion and heterogeneity (morphology) of blends on a molecular level. In this work, the compatibilization effects of linear low density polyethylene-*g*-polystyrene (LLDPE-*g*-PS) with different grafting yield on immiscible blends of linear low density polyethylene (LLDPE) and styrene–butadiene–styrene triblock copolymer (SBS) have been investigated by n.m.r. and d.s.c. techniques in order to explore the compatibilizing mechanism of LlDPE-*g*-PS on immiscible LlDPE/SBS blends on a molecular level.

EXPERIMENTAL

Graft copolymers with different PS grafting yield, LLDPE-

* To whom correspondence should be addressed. Present address: Max-Planck-Institut für Polymerforschung, Postfach 3148, D-55021 Mainz, Germany

g-PS, were synthesized in our laboratory. All operations were carried out under argon atmosphere using standard Schlenk techniques. Macromer PS-allyl was prepared with *n*-BuLi in the usual manner of styrene anionic polymerization, except that the polymerization was terminated with allyl bromide. The ethylene/1-hexene/PS-allyl terpolymerization was conducted in a manner similar to ethylene/1-hexane copolymerization[11] with Kaminsky catalyst system. $Me_2Si(Cp)_2ZrCl_2$/methylaluminoxane (MAO) at 50°C under 1.5 atm. ethylene pressure, with the macromer (w_1) having been dissolved in the polymerization medium toluene. The reaction was terminated by adding a few drops of acidified ethanol, and the polymerization mixture was washed with butanonic hydrochloride acid solution. The resulting polymer was collected by filtration and dried under vacuum to a constant weight (w_2). Ungrafted macromer (w_3) was obtained by weighing the filtrate of butanone. The grafting yield (Y) of the copolymer (LLDPE-*g*-PS) was calculated by:

$$Y\,(\%) = \frac{w_1 - w_3}{w_2} \times 100\% \qquad (1)$$

The characterization data of the copolymers are listed in *Table 1*.

SBS triblock copolymer was obtained from the Synthetic Rubber Factory of Baling Petrochemical Co. and was purified before use. LLDPE (T_m = 390 K) was obtained from Sumitomo Chemical Co. Ltd of Japan. Solution blending was used in this study, using toluene as solvent and a solution of concentration of 5% (w/v). The blends with different compositions, dissolved in the boiling toluene, were precipitated by pouring the solution into ethanol. Having been filtered, the products were washed with ethanol several times. The blends were dried at room temperature and then dried under vacuum to a constant weight. All blends were annealed under vacuum at 435 K for 30 min before being used for n.m.r. and d.s.c. experiments.

Solid state ^{13}C CPMAS n.m.r. experiments were performed on a Bruker MSL-400 n.m.r. spectrometer at 298 K. The TOSS method was used for suppressing spinning side bands. The carbon-13 resonance frequency was 100.63 MHz, and proton resonance frequency 400.13 MHz. Dipolar decoupling field was about 49 kHz. ^{13}C spectra were referred to the chemical shift of methyl group carbons of hexamethylbenzene which was 16.9 ppm.

The d.s.c. experiments were done using a Perkin-Elmer apparatus DSC-2 at a heating rate of 10 K min^{-1}.

RESULTS AND DISCUSSION

The ^{13}C–^{1}H heteronuclear dipolar dephasing technique may allow qualitative or quantitative discrimination among different chemical species, domains or phases[12,13]. *Figure 1* shows the dipolar dephasing spectra of LLDPE/SBS (70/30) blends with and without LLDPE-*g*-PS. The dipolar dephasing spectrum (*Figure 1*A(e)) of LLDPE/SBS blends contains two resonance peaks with equal intensities at 30.6 and 32.2 ppm. Obviously, the 32.2 ppm peak can be assigned to carbon resonance from crystalline domains of LLDPE, and the 30.6 ppm peak to carbon resonance from amorphous domains of LLDPE[14]. The addition of equal content (5 wt%) LlDPE-*g*-PS with different PS grafting yield to LLDPE/SBS blends gives rise to an obvious change of the dipolar dephasing spectra (*Figure 1*A(a)–(d)) of the blends. The relative intensity of the crystalline peak (33.3 ppm) becomes larger than that of the amorphous peak (30.6 ppm). At the same time, the relative intensity difference between the two peaks increases with the PS grafting yield of LlDPE-*g*-PS. The increase in the relative intensity of the crystalline peak suggests that the crystallites of LLDPE become less perfect or the relative content of less perfect crystallites of LLDPE increases due to the addition of LLDPE-*g*-PS. The rate of molecular motion in less perfect crystallites will be faster than that in relatively perfect crystallites, which contributes to the increase in the relative intensity of the crystalline peak. *Figure 1*B shows the dipolar dephasing spectra of the same specimens with much longer dephasing time (T_{DD} = 50 μs). Comparing *Figure 1*B with *Figure 1*A, there are several points worthy of note:

(1) the crystalline peak at 32.2 ppm disappears due to the strong dipole–dipole interactions among protons in the crystalline region;
(2) the addition of LLDPE-*g*-PS to LlDPE/SBS blends causes a marked increase in resonance intensity of the amorphous peak and obvious narrowing of the amorphous linewidth, which can also be seen from the marked increase in T_2(H) of the amorphous region (*Table 2*);

Table 1 Characterization data of grafting copolymers LLDPE-*g*-PS

No.	PS grafting yield in LLDPE-*g*-PS (wt%)	$M_w \times 10^{-4}$	Designation
1	2.0	8.09	GPS2
2	2.9	1.26	GPS3
3	3.6	0.87	GPS4
4	13.0	2.56	GPS13
5	17.0	–	GPS17
6	16.8	2.80	HGPS17[a]
7	27.0	4.88	GPS27

[a] Ethylene/PS-allyl copolymer.

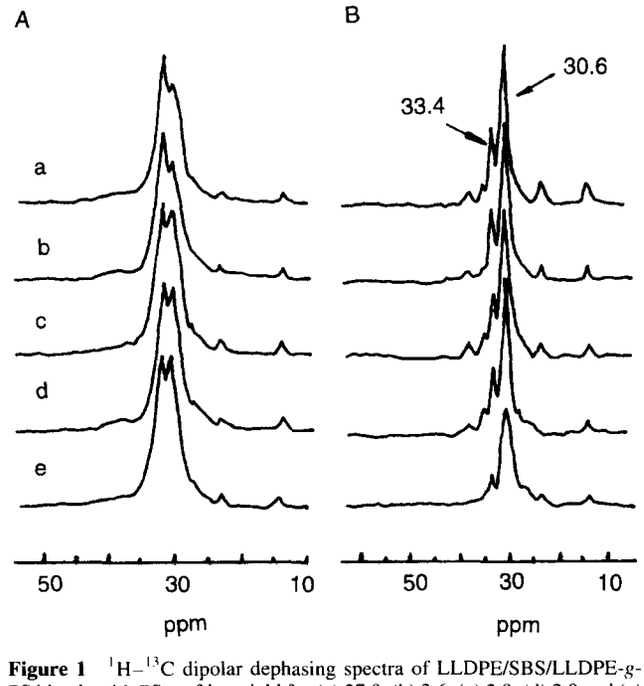

Figure 1 ^{1}H–^{13}C dipolar dephasing spectra of LLDPE/SBS/LLDPE-*g*-PS blends with PS grafting yield for (a) 27.0, (b) 3.6, (c) 2.9, (d) 2.0 and (e) 0 wt%. The dipolar dephasing times (T_{DD}) are: T_{DD} = 4 μs for A and T_{DD} = 50 μs for B

Table 2 Effect of PS grafting yield in LLDPE-*g*-PS on $T_2(H)^a$ (μs) and $T_{1\rho}(H)^a$ (ms) values of LLDPE/SBS (70/30) blends

Specimen	Peak at 32.3 ppm				Peak at 30.6 ppm			
	$T_{1\rho}(H)$	%	$T_{1\rho}(H)$	%	$T_2(H)$	%	$T_2(H)$	%
LLDPE/SBS	5.8	50.2	1.8	49.8	112	43.7	13	56.3
LLDPE/SBS/GPS2[b]	14.3	34.2	3.2	65.8	194	33.2	12	66.8
LLDPE/SBS/GPS4	9.9	41.8	2.3	58.2	272	31.5	12	68.5
LLDPE/SBS/GPS17	8.7	47.5	1.9	52.5	248	31.9	13	68.1
LLDPE/SBS/GPS27	7.8	12.9	2.3	87.1	231	39.2	12	60.8

[a] Estimated error $\leq \pm 5\%$.
[b] The content of LLDPE-*g*-PS in all the blends is 5% by weight.

Table 3 Effect of LLDPE-*g*-PS content on $T_2(H)^a$ (μs) and $T_{1\rho}(H)^a$ (ms) values of LLDPE/SBS (70/30) blends

LLDPE-*g*-PS (GPS4)	Peak at 32.3 ppm				Peak at 30.6 ppm			
	$T_{1\rho}(H)$	%	$T_{1\rho}(H)$	%	$T_2(H)$	%	$T_2(H)$	%
0	5.8	50.2	1.8	49.8	112	43.7	13	57.3
3	9.5	50.4	2.4	49.6	587	26.3	15	73.7
7	8.4	56.6	2.2	43.4	–	–	–	–
10	10.7	62.8	1.9	37.2	336	31.0	15	69.0

[a] Estimated error $\leq \pm 5\%$.

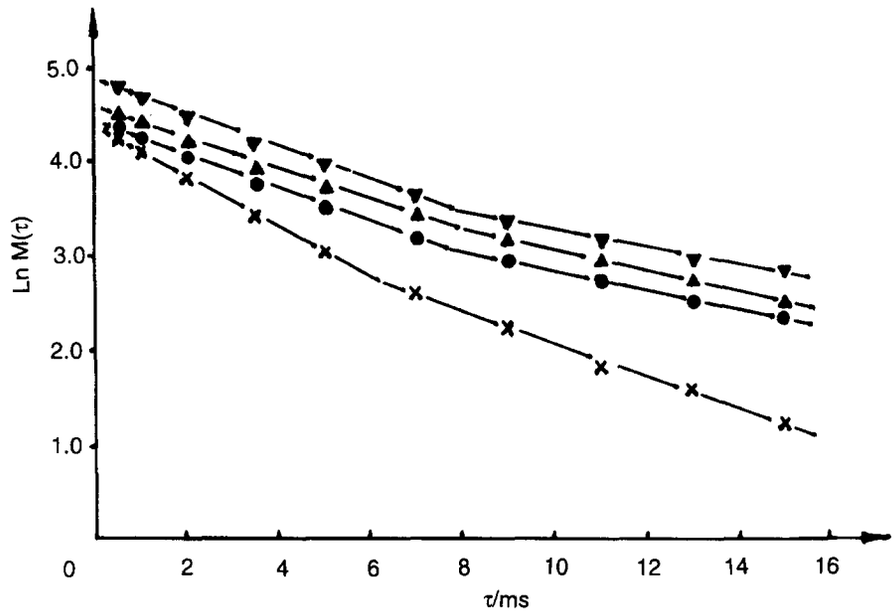

Figure 2 Logarithmic intensity of the CPMAS ^{13}C spectra of LLDPE/SBS/LLDPE-*g*-PS blends vs. proton spin-locking time with PS grafting yield for: 0 (×), 2.0 (●), 3.6 (▲) and 27.0 wt% (▼)

(3) a new resonance peak appears at 33.4 ppm due to the addition of LLDPE-*g*-PS, and its relative intensity increases with the PS grafting yield of LLDPE-*g*-PS. This new resonance peak may be ascribed to the less perfect crystallites in which LLDPE chains have quite different conformation from those in perfect crystallites and those in the amorphous region. It is this resonance peak which is mainly responsible for the increase in the relative intensity of the crystalline peak mentioned above due to overlapping with the crystalline peak.

From the results mentioned above, it can be clearly seen that the addition of LLDPE-*g*-PS to LLDPE/SBS blends has an obvious effect on the crystallization behaviour of LLDPE, increasing the relative content of less perfect crystallites and causing the amorphous region to become more mobile. This conclusion is further supported by results from d.s.c., proton and carbon-13 spin–relaxation measurements of the same specimens.

The values of $T_{1\rho}(H)$ listed in *Tables 2 and 3* were obtained from the decay of the ^{13}C CPMAS intensity with proton spin-locking time[15]. *Figure 2* shows the $T_{1\rho}(H)$ relaxation of LLDPE in LLDPE/SBS blends with and without LLDPE-*g*-PS. From *Table 2* and *Figure 2* it can be seen that: (1) there exist two $T_{1\rho}(H)$ values for the crystalline peak (32.2 ppm) and (2) the addition of LLDPE-*g*-PS to

LLDPE/SBS blends gives rise to effects on the two $T_{1\rho}$(H) values to different degrees. As is well known, a single $T_{1\rho}$(H) value has been used as a criterion for the miscibility or homogeneity of multicomponent polymer systems. The two $T_{1\rho}$(H) values found in the crystalline region indicate heterogeneity. A reasonable explanation for the existence of heterogeneity in the crystalline region is that a perfect crystalline region and a less perfect crystalline region coexist in the crystalline region of LLDPE. Generally, the species in relatively mobile region will have shorter $T_{1\rho}$(H) and a longer $T_{1\rho}$(H). Hence, the chains with longer $T_{1\rho}$(H) could be assigned to the perfect crystalline region, and those with shorter $T_{1\rho}$(H) to the less perfect crystalline region mentioned above. The addition of LLDPE-*g*-PS to LLDPE/SBS blends makes the longer $T_{1\rho}$(H) become even longer and the shorter one almost unchanged. At the same time, the relative content of the longer $T_{1\rho}$(H) component decreases due to the addition of LLDPE-*g*-PS. It was found that the T_1(C) and $T_{1\rho}$(H) values of semicrystalline polymers increase with their crystallite thickness[16,17]. Hence, the increase in $T_{1\rho}$(H) values of LLDPE may also result from the increase in the crystallite thickness. Here, it should be pointed out that the increase in crystallite thickness does not require an increase in crystallinity or an increase in the relative content of the perfect crystalline component. In fact, in this case the relative content of the perfect crystalline component decreases due to the addition of LLDPE-*g*-PS.

The effect of LLDPE-*g*-PS on the amorphous region of LLDPE is also marked. The $T_{1\rho}$(H) values of the amorphous region of LLDPE are too small to be detected. Fortunately, their T_2(H) values are longer and easily obtained. The T_2(H) values of the blends are listed in *Table 2*. Interestingly, there also exist two T_2(H) values for all the blends. Naturally, the longer T_2(H) value belongs to the amorphous region or liquid-like region, and the shorter one can be assigned to the non-crystalline intermediate region, i.e. interfacial region. It was found that the T_2(H) of the amorphous region increases greatly but the relative content of the amorphous region decreases due to the addition of LLDPE-*g*-PS. The T_2(H) value of the interfacial region remains unchanged in spite of the increase in relative content of the interfacial region.

The results mentioned above allow us to draw the following conclusions: the addition of LLDPE-*g*-PS to LLDPE/SBS (70/30) blends leads to an enlarging of the interfacial region, an increase in the motion freedom of the amorphous region, an increase in crystalline thickness, and a decrease in the relative content of the perfect crystalline component of LLDPE. The effect of LLDPE-*g*-PS on the crystallization behaviour of LLDPE has almost no dependence on the PS grafting yield of LLDPE-*g*-PS under the studied range (2.0–27.0 wt%). This may be related to the fact that for random branching copolymer, branch-free segments may be incorporated within lamellae and the portions of concentrated branching within the same molecule rejected to the interlamellar region[18]. The latter contributes to the increase in the relative content of less perfect crystalline region, the enlarging of the interfacial region and the increase in motion freedom of the amorphous region.

The effect of content of LLDPE-*g*-PS on $T_{1\rho}$(H) and T_2(H) values of LLDPE in the blends are marked (see *Table 3*). It is easy to see that the addition of a small quantity of LLDPE-*g*-PS ($\geq$ 3 wt%) to LLDPE/SBS blends will give rise to obvious effects on both the $T_{1\rho}$(H) and T_2(H) values of LLDPE, i.e. the crystallization behaviour of LLDPE.

To investigate the compatibilization effect of LLDPE-*g*-PS on LLDPE/SBS blends, it is not enough to know the effect of LLDPE-*g*-PS on the crystallization behaviour of LLDPE. We also have to know how the compatibilizers influence the microstructure of the other component, SBS, of the blends. ^{13}C spin–lattice relation time (T_1(C)) has been used to characterize molecular motion in semicrystalline polymers[16,19]. Usually, carbons in the crystalline (or rigid) region will have much longer T_1(C) values than those in the amorphous (or mobile) region[16]. The effect of LLDPE-*g*-PS on T_1(C) values of both the components, LLDPE and SBS, of the blends with different compositions are drastic (see *Table 4*). There are several points concerning the data in *Table 4* which are worth mentioning. First, the addition of LLDPE-*g*-PS to LLDPE/SBS blends causes an obvious decrease in the T_1(C) values of PS blocks and leads to a change in the T_1(C) relaxation of PS blocks from exponential to exponential. When the content of LLDPE-*g*-PS in the blends is kept constant, the smaller the content of LLDPE in the blends the more serious the effect of LLDPE-*g*-PS on T_1(C) values of PS blocks. These results indicate that parts of LLDPE-*g*-PS added are soluble into the domains of PS blocks. The presence of two T_1(C) values for PS blocks suggests that a heterogeneous structure, including a bulk region and an interfacial region in PS block domain, occurs due to the addition of LLDPE-*g*-PS. In addition, the interfacial region contains about half of the total PS blocks. It was found that the shorter T_1(C) value of PS blocks is equal to the amorphous T_1(C) value of LLDPE. This means that the PS block chains in the interfacial region move cooperatively with the LLDPE chains in the amorphous region. It is the 'bridge' role of LLDPE-*g*-PS that makes such a cooperative motion between the immiscible components possible. Secondly, the addition of LLDPE-*g*-PS into LLDPE/SBS blends simultaneously gives rise to a marked effect on the T_1(C) values of LLDPE. For instance, the crystalline T_1(C) value of LLDPE in the LLDPE/SBS (50/50) blends decreases from 87.3 to 48.0 s due to the addition of 5 wt% LLDPE-*g*-PS. At the same time, the corresponding content of the crystalline component changes from 62.7 to 8.9%. It was found that the

Table 4 Effect of LLDPE-*g*-PS on T_1(C) (s) values of LLDPE/SBS blends

LLDPE/SBS/GPS17	PS block in SBS (40.7 ppm)				LLDPE (32.3 ppm)			
	T_1(C)	%	T_1(C)	%	T_1(C)	%	T_1(C)	%
0/100/0	32.4	100						
100/0/0					113.6	54.8	0.7	45.2
50/50/0	16.9	100			87.3	62.7	0.4	37.3
47.5/47.5/5	7.1	44.6	0.2	55.4	48.0	8.9	0.41	91.1
30/70/0	32.0	100			0.2	100		
28.5/66.5/5	5.6	52.2	0.6	47.8	0.3	100		

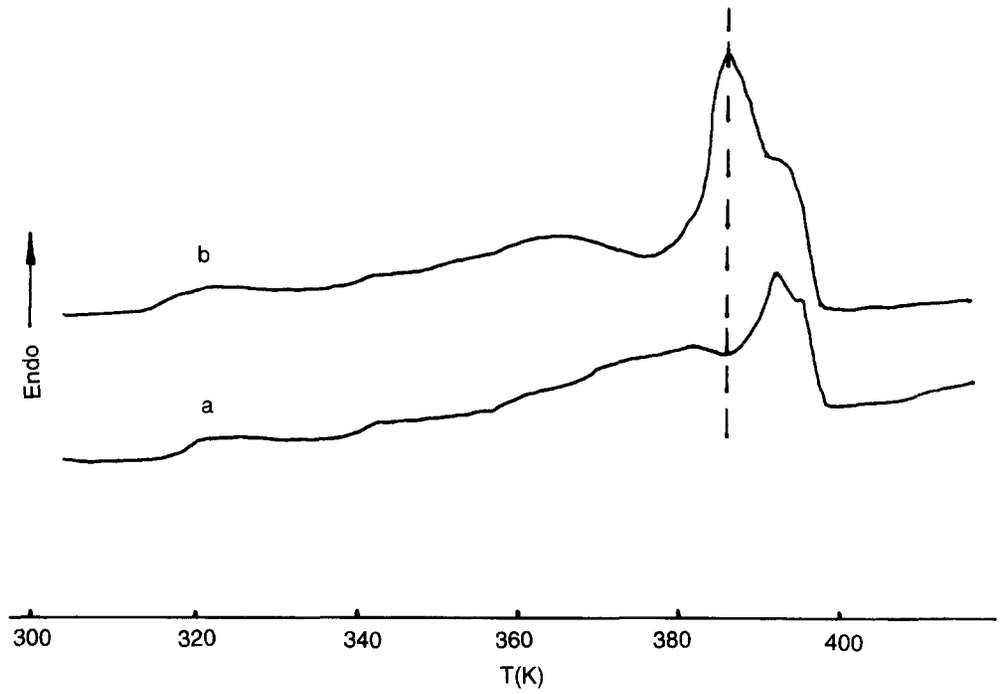

Figure 3 Melting curves of blends for: (a) LLDPE/SBS (50/50), (b) LLDPE/SBS/LLDPE-*g*-PS (47.5/47.5/5)

crystalline T_1(C) values of PE have a one-to-one relation with the crystallite thickness, and the changes in the interfacial structure can also have a drastic effect on the crystalline T_1(C) values [16]. Without doubt, the decrease in the crystalline T_1(C) values of LLDPE originates from both the decrease in the crystallite thickness and the widening of the interfacial region of LLDPE. This conclusion is further supported by the results from d.s.c. measurements of the same specimens. Shown in *Figure 3* are the typical melting curves of LLDPE/SBS (50/50) blends with and without LLDPE-*g*-PS. It is clear that a great quantity of low melting point crystallites formed as a result of the addition of LLDPE-*g*-PS. Here, it should be pointed out that the effect of LLDPE-*g*-PS on the crystallization behaviour of LLDPE in LLDPE/SBS depends on the composition of the blends. Finally, the effect of LLDPE-*g*-PS on the domain size of LLDPE was detected by means of proton spin–diffusion experiments[20]. Usually, the maximum diffusive path length X during time t can be calculated by the following equation[21]:

$$< X >^2 = 6Dt \tag{2}$$

where D is the spin diffusion coefficient, which can be calculated by[22]

$$D = 2r_0^2/T_2 \tag{3}$$

where T_2 is the spin–spin relaxation time of the more mobile components and the hydrogen von der Waals radius of 1.17 Å is used for r_0[23]. Having obtained the values of T_2 and t of the studied systems, one can use the above equations to calculate the domain size.

The results listed in *Table 5* are the domain sizes, measured by proton spin diffusion, of LLDPE in LLDPE/SBS blends with and without LLDPE-*g*-PS. It is clearly seen that the domain size of LLDPE decreases a lot because of the addition of LLDPE-*g*-PS. At the same time it is also found that LLDPE-*g*-PS with PS grafting yield more than 2 wt% can efficiently reduce the domain size of LLDPE. Hence, we can exclude the possibility that the marked effect of LLDPE-*g*-PS on both the crystallization behaviour of LLDPE and the microstructure of SBS may result from the solubilization of LLDPE-*g*-PS into the LLDPE and SBS domains, which will enlarge the domain sizes of LLDPE and SBS. From the results mentioned above, the following conclusions can be drawn.

(1) LLDPE-*g*-PS is a good compatibilizer for LLDPE/SBS blends. A good compatibilization effect on LLDPE/SBS blends can be achieved when the content of LLDPE-*g*-PS in the blends is greater than 3 wt%.
(2) The possible mechanism of LLDPE-*g*-PS compatibilizing immiscible LLDPE/SBS blends is that LLDPE-*g*-PS connects two immiscible components, LLDPE and SBS, through solubilization of chemically identical segments in LLDPE-*g*-PS into the amorphous region of LLDPE and PS block domains of SBS, respectively. At the same time, parts of LLDPE chains free-branching in LLDPE-*g*-PS connect with crystalline phase of LLDPE by isomorphism, which has a serious effect on the crystallization behaviour of LLDPE. As a consequence, the crystallite thickness of LLDPE decreases sharply and a large quantity of less perfect crystallites forms.
(3) A new interfacial region rich in LLDPE-*g*-PS between SBS domains and LLDPE domains forms due to the addition of LLDPE-*g*-PS. It is estimated that half of the total PS blocks locate at this interfacial region.

Table 5 Effect of PS grafting yield in LLDPE-*g*-PS on domain size of LLDPE in LLDPE/SBS (70/30) blends

Specimen	T_2 (μs)	SD time (ms)	Domain size (Å)
LLDPE/SBS	112	284	204.0
LLDPE/SBS/GPS2[a]	194	409	186.0
LLDPE/SBS/GPS4	272	239	120.0
LLDPE/SBS/GPS17	248	186	111.0
LLDPE/SBS/GPS27	231	189	116.0

[a] The content of LLDPE-*g*-PS in all the blends is 5% by weight.

Finally, it should be pointed out that the ^{13}C spectra of LLDPE in all the blends consist of two peaks at 32.3 ppm and 30.6 ppm, respectively, and their chemical shifts have little dependence on the blend compositions. However, the spin relaxation times of LLDPe in all the blends, which reflect crystallization behaviour or supermolecular structure of LLDPE, obviously depend on the composition of the blends, and the results from spin relaxation times are in excellent agreement with those from d.s.c. measurements. Therefore, spin relaxation times are better parameters than ^{13}C chemical shifts in determining supermolecular structure of polymers.

ACKNOWLEDGEMENTS

The authors are grateful for the financial support granted by the National Natural Science Foundation of China, the Laboratory of Magnetic Resonance and Atomic and Molecular Physics, Wuhan Institute of Physics, Chinese Academy of Sciences.

REFERENCES

1. Rayt, R., Jerome, R. and Teyssie, Ph., *Journal of Polymer Science, Polymer Physics Edition*, 1982, **20**, 2209.
2. Heikens, D., Hoen, N., Barentsen, W., Piet, P. and Ladan, H. J., *Polymer Science, Polymer Symposia*, 1978, **62**, 309.
3. Boutevin, B., Pietrasanta, Y., Taha, M. and Sarraf, T., *Polymer Bulletin*, 1985, **14**, 25.
4. Ouhadi, T., Fayt, R., Jerome, R. and Teyssie, Ph., *Journal of Applied Polymer Science*, 1986, **32**, 5647.
5. Ide, F. and Hasegawa, A. J., *Applied Polymer Science*, 1974, **18**, 963.
6. Anastasiadis, S. H., Gancarz, I. and Koberstein, J. T., *Macromolecules*, 1989, **22**, 1449.
7. Wu, S., *Polymer Engineering and Science*, 1987, **27**, 335.
8. Fayt, R., Jerome, R. and Teyssie, P., *Makromolekulare Chemie*, 1986, **187**, 837.
9. Noolandi, J. and Hong, K. M., *Macromolecules*, 1984, **17**, 1531.
10. Datta, S. and Lohse, D. J., *Macromolecules*, 1993, **26**, 2064.
11. Doivumaki, J. and Seppala, J. V., *Macromolecules*, 1993, **26**, 5535.
12. Opella, S. J. and Frey, M. H., *Journal of the American Chemical Society*, 1979, **101**, 5854.
13. Wilson, M. A., Pugmire, R. J., Alemany, L. B., Woolfenden, W. R., Grant, D. M. and Given, P. H., *Analytical Chemistry*, 1984, **56**, 933.
14. Kitamaru, R., Horri, F. and Murayama, K., *Macromolecules*, 1986, **19**, 636.
15. Stejskal, E. O., Schaefer, J., Sefcik, M. D. and Mckay, R. A., *Macromolecules*, 1981, **14**, 275.
16. Axelson, E. E., Mandelkern, L., Popli, R. and Mathieu, P., *Journal of Polymer Science, Polymer Physics Edition*, 1983, **21**, 2319.
17. Packer, K. J., Polett, I. J. F. and Taylor, M. J. J., *Chemical Society, Faraday Transactions* 1988, I, **84**, 3851.
18. Bassett, D. C., *Principles of Polymer Morphology*. Cambridge University Press, Cambridge, 1981, p. 120.
19. Fedotov, V. D. and Schneiderm, H., *Structure and Dynamics of Bulk Polymers of NMR-Methods*. Springer, Berlin, 1989.
20. Tekely, P., Canet, D. and Puech, J., *Journal of Molecular Physics*, 1989, **67**, 81.
21. Tanaka, H. and Nishi, T., *Physics Reviews*, 1986, **B33**, 32.
22. Shibayama, M. and Hashimoto, T., *Macromolecules*, 1986, **19**, 740.
23. Assink, R. A., *Macromolecules*, 1978, **11**, 1233.